Influence of heat treatment and hot working on fracture toughness of cast aluminium base composites

L. Wei and J. C. Huang

Evaluation of toughness in terms of the fracture energy E^*, obtained using Charpy impact testing and the fracture toughness K_{Ic}, obtained from bend tested specimens, has been carried out for various cast particle reinforced aluminium base composites, namely, A356–SiC, A357–SiC, 6061–Al_2O_3, and 2014–Al_2O_3. In practice, the first two are used in the as cast foundry condition and the last two in the cast and extruded condition. Hot extrusion or rolling to reduction ratios between 2 : 1 and 50 : 1 was conducted on the 6061 and 2014 composites to characterise the influence of working processes. Heat treatment conditions considered included the as cast (or as worked), solid solution treated, and T6 temper. The results show that extrusion or rolling can markedly improve the toughness, but on thermal aging the toughness is reduced. The increase in total fracture energy by hot working is mainly caused by the increase of initiation energy, whereas the decrease of fracture energy by artificial aging is controlled by the propagation energy. The values of K_{Ic} obtained for these composites are from 15 to 25 MN m$^{-3/2}$. Comparisons and interpretations of the dynamic Charpy fracture energy, quasistatic fracture toughness, and fracture surface of the four composites are also presented. MST/1806

 Manuscript received 23 November 1992; in final form 11 Feburary 1993. *The authors are at the Institute of Materials Science and Engineering, National Sun Yat-Sen University, Kaohsiung, Taiwan.*

Introduction

Aluminium base metal matrix composites (MMCs) have attracted considerable interest recently since they offer the opportunity to tailor a material with a combination of strength (or modulus)/density ratio and wear properties superior to most metal alloys. Reinforcement in the form of long fibres, short whiskers, and particles, typically SiC or Al_2O_3, can be added to various commercial aluminium alloys, such as A356 (or A357),[1,2] 2000,[3] 6000,[4] or 7000[5] series. The volume fraction and size of reinforcement usually lie in the range 10–30% and 1–20 μm, respectively.

Recent developments have increased the range from the original long fibre reinforced systems (such as Al–B) to particle and whisker reinforced materials. The work on cast MMCs has resulted in a type of composite which is much more economically feasible than previous MMCs and could compete with metallic materials in terms of properties as well as cost. However, whether cast or produced via powder metallurgy, the lack of toughness, ductility, and formability still limits the industrial applications of these materials.

The toughness of MMCs can be controlled by varying the material and processing parameters, such as type, shape, aspect ratio, volume fraction, orientation, and distribution of reinforcement, as well as the matrix and interfacial properties, which can include solute segregation, precipitation, porosity, residual stress, interfacial bonding strength, original sample surface roughness, etc. Most of these parameters will be strongly influenced by the processing and thermal treatment history. It can thus be seen that to evaluate the fracture toughness of a MMC is not simple.

Friend[6] has reviewed the results on the toughness of aluminium MMCs with both continuous and discontinuous reinforcements. In his paper, the emphasis was on the definition and measurement of MMC toughness, including fracture toughness K_{Ic} and Charpy fracture energy E^*. The K_{Ic} measurement can be performed either quasistatically (strain rate of $\sim 10^{-3}$ s^{-1}) or dynamically ($>10^2$ s^{-1}, which may be termed K_{ID}). Although the fracture toughness and fracture energy differ in physical meaning, they both can and have been used to characterise the toughness. A relationship between E^* and K_{Ic} has been proposed,[7,8] but the meaning is still debatable. By analysing the data in the literature, Friend suggested combining the measurements of fracture toughness and fracture energy in order to characterise the complete fracture response.[6]

The present research was carried out in an attempt to characterise the fracture toughness more systematically by using various commercially available aluminium based MMCs fabricated via the low cost cast route. Material variables under examination include: aluminium alloy matrix, heat treatment, condition of ceramic reinforcements, and fabrication history.

Experimental methods

MATERIALS

The particle reinforced composites used were A356–SiC, A357–SiC, 6061–Al_2O_3, and 2014–Al_2O_3, supplied in the as cast condition by the Duralcan Company, USA. The compositions and particle data are given in Table 1. It should be noted that the first two composites are generally used in their as cast or recast condition, whereas the last two are used in the cast and extruded condition. The present study of fracture toughness followed these two categories of treatment history, so the results will have practical meaning. Although all four materials were studied, the emphasis is on the 6061 composite. The other three were characterised mainly for comparison, to provide a more general concept of the fracture mechanisms.

MATERIAL TREATMENTS

All four materials were received in the as cast condition. The 6061 and 2014 composites were subjected to hot working processes including hot extrusion and rolling. The 6061 composite was first machined to rod of 100 or 150 mm dia. These were extruded at 500°C to a final diameter of 30 mm, corresponding to reduction ratios of 11 : 1 and 25 : 1, respectively. Before extrusion, the composite and extrusion die were preheated at 500°C for 2 h. The 2014 composite was extruded only to a reduction ratio of 36 : 1 owing to the limitations imposed by the size and properties of the as received materials. This composite was first machined to 90 mm rod, then preheated at 460°C for

Table 1 Chemical compositions and particle data for particle reinforced metal matrix composites (Al based) used in present work

Matrix composition, wt-%								Reinforcing particles				
Si	Mg	Cu	Fe	Ti	Be	Zn	Mn	Size *d*, μm	Aspect ratio	V_f, %	L_s,* μm	$L_s - 2r$, μm
A356–SiC												
7·0	0·4	0·2	0·15	0·2	...	...	0·1	~12·5	~2:1	20	20·2	7·7
A357–SiC												
7·0	0·55	0·1	0·1	0·2	0·06	...	0·05					
6061–Al_2O_3												
0·6	1·0	0·3	0·7	0·15	...	0·25	0·15	~19·0	~2:1	15	35·5	16·5
2014–Al_2O_3												
0·9	0·5	4·5	0·7	0·15	...	0·25	0·8					

* Approximate centre to centre spacing $L_s = r(2\pi/3V_f)^{1/2}$, where *r* is radius and V_f is volume fraction.

4·5 h and extruded at the same temperature to rod of 15 mm dia. For both types of composite, the extrusion speed was 5 mm s^{-1} and air cooling was applied after extrusion.

To explore further the effect of hot working, rolling was also performed using the 6061 composite. The as received materials were machined to rectangles having the dimensions 116 (length) × 41 (width) × 56·5 mm (height). Hot rolling to reduction ratios of 2:1 and 4:1 was conducted at 500°C. The materials were preheated at 500°C for 1 h, then rolled for five passes followed by reheating for 20 min, each pass to a reduction of 0·3 mm in thickness. The final thicknesses of the rolled plates were 28 and 14 mm, respectively. In addition, hot rolling was applied to the as extruded (25:1) 6061 composite, which was machined to 28 mm thickness and then hot rolled to 14 mm, resulting in a total reduction ratio of 50:1 from extrusion plus rolling. For this composite, the effects of different working paths and reduction ratios, 2:1, 4:1, 11:1, 25:1, and 50:1, were thus evaluated and compared.

Thermal heat treatments performed for the as cast and as worked composites included solid solution treatment (SS) at 500–540°C in salt bath and aging at 160°C (A356 and 2014 composites) or 170°C (A357 and 6061 composites) for 1, 5, 9, and 15 h in oil bath. These times were found to comprise the underaged to early overaged conditions for these composites. The peak aged condition was determined according to Vickers microhardness with 1 kg load and 5 s contact. The hardness tests were performed on the matrix material, avoiding the reinforcing particles; each value quoted represents the average of ten measurements.

MECHANICAL TESTING

The fracture toughness properties were studied in terms of fracture energy E^* and stress intensity factor in plane strain mode K_{Ic}. The fracture energy E^* was quantified by impact testing using standard sized (55 mm length) Charpy V-notched (CVN) or unnotched specimens under dynamic high loading rate conditions at ~4×10^2 s^{-1}. The extrusion or rolling direction is parallel to the longitudinal axis of the specimen and perpendicular to the notch. An instrumental 30 kg m Shimadzu Charpy testing system was used, with strain gauge equipped tup, Kyowa conditioner, plus HP recorder and controller. The sampling rate was 4×10^6 s^{-1}. The total fracture energy E^* has components of initiation energy E_i and propagation energy E_p during the fracture process, which are usually defined as the energy contributions before and after peak load F_p.

Values of K_{Ic} were measured from chevron notched specimens made following ASTM E399 specifications. The specimens were bend tested under quasistatic or low loading rate conditions at ~10^{-3} s^{-1}. The extrusion or rolling direction is again parallel to the longitudinal axis of the specimen. A precrack was produced by low cycle fatigue performed using an Instron 1332 system. To determine K_{Ic}, ASTM specifications were strictly followed; values otherwise obtained can be considered only as K_Q. Tensile tests were also conducted using a screw driven Instron 1125 machine at a strain rate of 1×10^{-3} s^{-1}. The stress data were used to evaluate the measured stress intensity factors as K_{Ic} or K_Q.

MICROSTRUCTURAL CHARACTERISATION

The particle distribution was first examined using optical microscopy (OM). The fracture surface is characterised by scanning electron microscopy (SEM). The results are compared with the data on E^* and K_{Ic}.

Results

OPTICAL MICROSCOPY

Typical microstructures of specimens of the four as cast composites are shown in Fig. 1; it can be seen that the distribution of reinforcing particles was macroscopically uniform. However, some indications of local clustering can be observed. The grain size of the AC specimens was found to be of the same order as the interparticle spacing (Table 1) and the distribution was rather scattered. After extrusion/rolling, the massive particle clusters in the 6061 and 2014 composites were dispersed much more uniformly, but with some indications of preferential alignment along the working direction (e.g. *see* Fig. 2). Materials worked to higher reduction ratios had particles of smaller average size (values are given in Table 2). This was particularly apparent in the 2014 composite, presumably due to the higher matrix strength (compared with the 6061 alloy),

Table 2 Average particle size and particle spacing of as cast (AC) and hot rolled and/or extruded composites

Parameter, μm	AC	Reduction ratio					
		Hot rolled (HR)		Extruded (E)			HR + E
		2:1	4:1	11:1	25:1	36:1	50:1
6061–Al_2O_3							
d	19·0	18·0	18·0	17·0	16·0	...	16·0
L_s	35·5	33·6	33·6	31·9	29·9	...	29·9
$L_s - 2r$	16·5	15·6	15·6	14·8	13·9	...	13·9
2014–Al_2O_3							
d	19·0	...	...	...	...	13·0	...
L_s	35·5	...	...	...	...	24·3	...
$L_s - 2r$	16·5	...	...	...	...	11·3	...

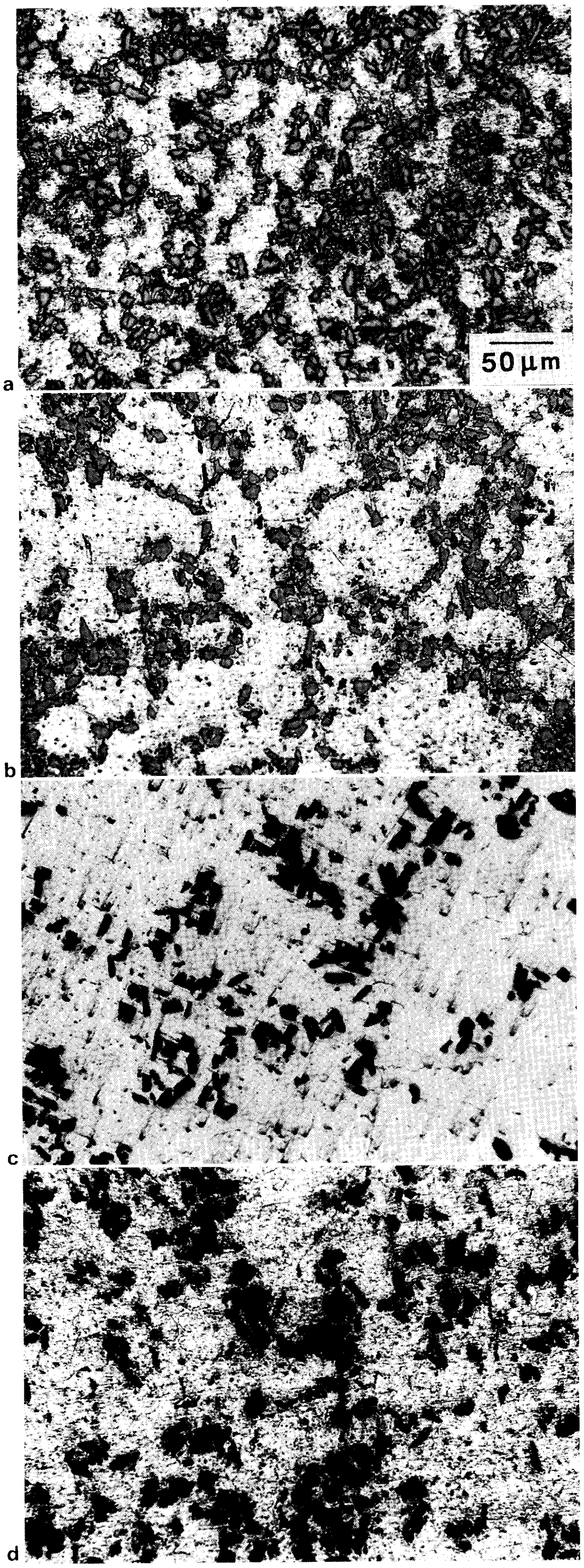

a A356–SiC; *b* A357–SiC; *c* 6061–Al_2O_3; *d* 2014–Al_2O_3

1 Microstructures of as cast (AC) specimens of particle reinforced metal matrix composites (OM)

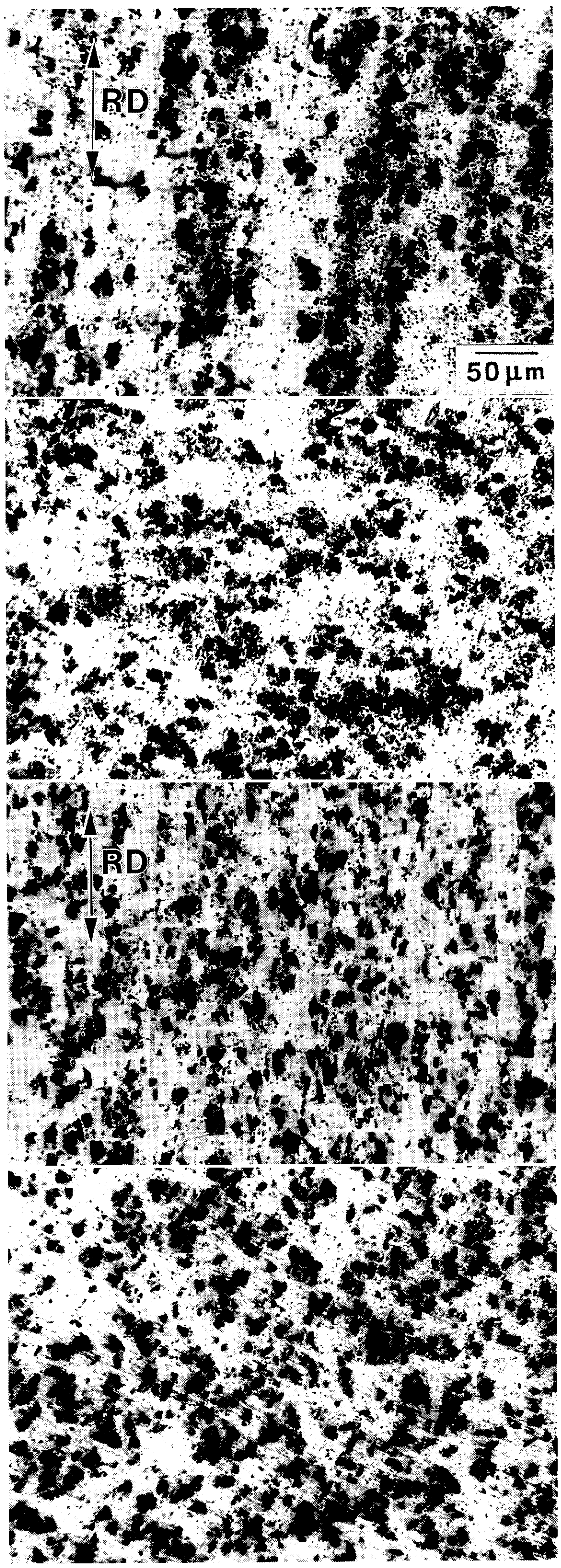

a, c surface parallel to rolling direction; *b, d* surface perpendicular to rolling direction

2 Microstructures of as worked (AW) specimens of Al_2O_3 particle reinforced *a, b* 6061 (25:1) and *c, d* 2014 (36:1) composites (OM)

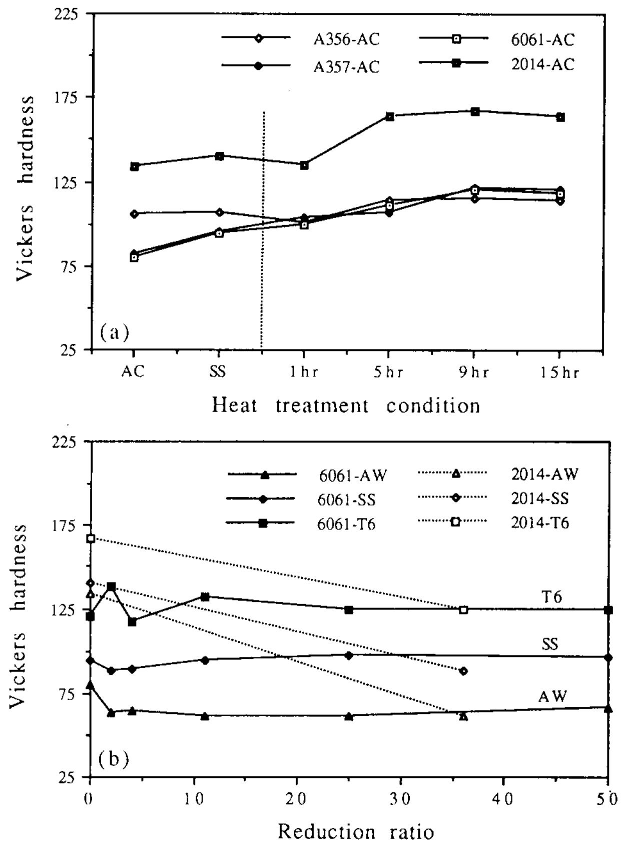

AC as cast; AW as worked; SS solid solution treated

3 Variation of Vickers hardness (HV1) of composites with *a* heat treatment and *b* hot working reduction ratio

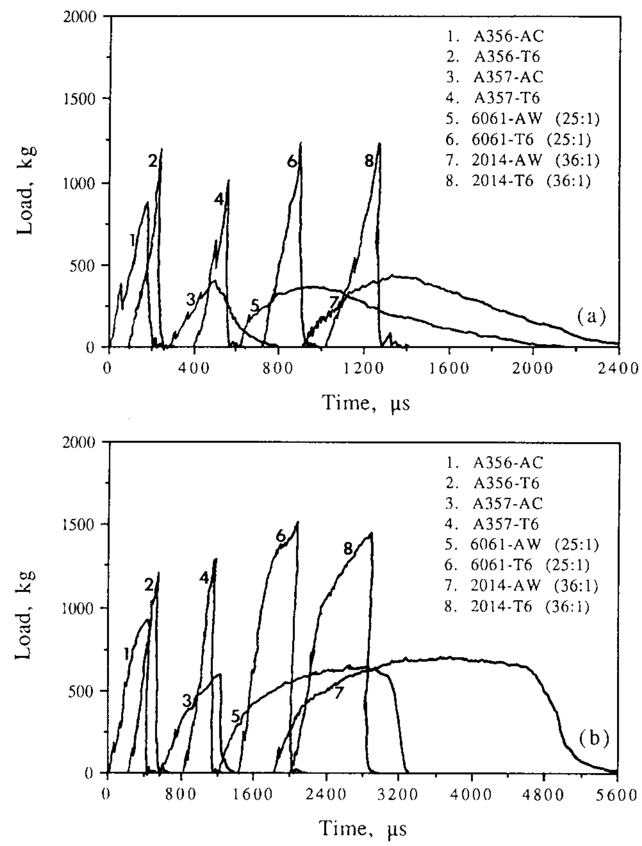

4 Representative Charpy response curves for *a* V-notched and *b* unnotched composite specimens

which results in the particles being more severely fractured during working.

MICROHARDNESS AND TENSILE MEASUREMENTS

Results from microhardness measurements suggest that the composites achieve the peak age (T6) condition after ~9 h at 160 or 170°C, as shown in Fig. 3*a*. The variation of hardness for the heat treated 6061 and 2014 composites after hot working is shown in Fig. 3*b*. The values for the T6 tempered 6061 composite appear not to be strongly affected by working, but there was a noticeable effect on the 2014 composite. The rather high hardness of the as cast 2014 composite may be due to a rapid cooling rate used by the fabricator (this is supported by the results of Ferry *et al.*[9]); the dislocations thereby induced tend to strengthen particle reinforced MMCs. In the present study, air cooling was carried out after hot working.

The data on the strength and elongation of the composites are given in Table 3, together with data for the unreinforced alloys. It can be seen that the strength and elongation levels for the AW or AW + T6 6061 and 2014 composite are significantly higher than for the AC A356 and A357 composites. The work done *W* (area under the true stress–true strain curves after unit transformation) for these two categories of composites is about 100–300 and 15–30 kJ m^{-2}, respectively. These data alone suggest a much improved toughness of the worked composites. Since the volume fraction (15 and 20%) and the type (Al_2O_3 and SiC) of reinforcing particles in these two composite systems differ, the influence from these factors is difficult to assess in this study and will not be discussed here.

Table 3 Tensile properties of matrix alloys and of particle reinforced composites

Material	Reduction ratio	Yield strength, MN m^{-2}		Ultimate tensile strength, MN m^{-2}		Elastic modulus in T6 condition, GN m^{-2}	Elongation, %		Work done *W*, kJ m^{-2}	
		AC/AW†	T6	AC/AW	T6		AC/AW	T6	AC/AW	T6
A356 alloy	...	...	200	...	276	72	...	15·0	...	...
A356–SiC	...	225	268	231	297	96	1·3	0·7	28	19
A357 alloy	...	...	347	...	396	72	...	8·6	...	...
A357–SiC	...	155	288	166	304	97	1·0	0·7	16	20
6061 alloy	...	...	280	...	314	70	...	20·0	...	...
6061–Al_2O_3	2:1	126	317	146	338	...	10·7	3·2	138	99
	4:1	140	334	163	373	...	12·8	5·1	184	171
	11:1	128	340	160	357	...	23·6	5·8	320	192
	25:1	143	318	168	356	87	10·8	5·7	159	183
	50:1	137	340	161	360	...	10·0	4·7	141	156
2014 alloy	...	...	480	...	510	73	...	13·0	...	...
2014–Al_2O_3	36:1	...	480	...	530	92	...	2·3	...	110

† Tested in the AC or AW condition.

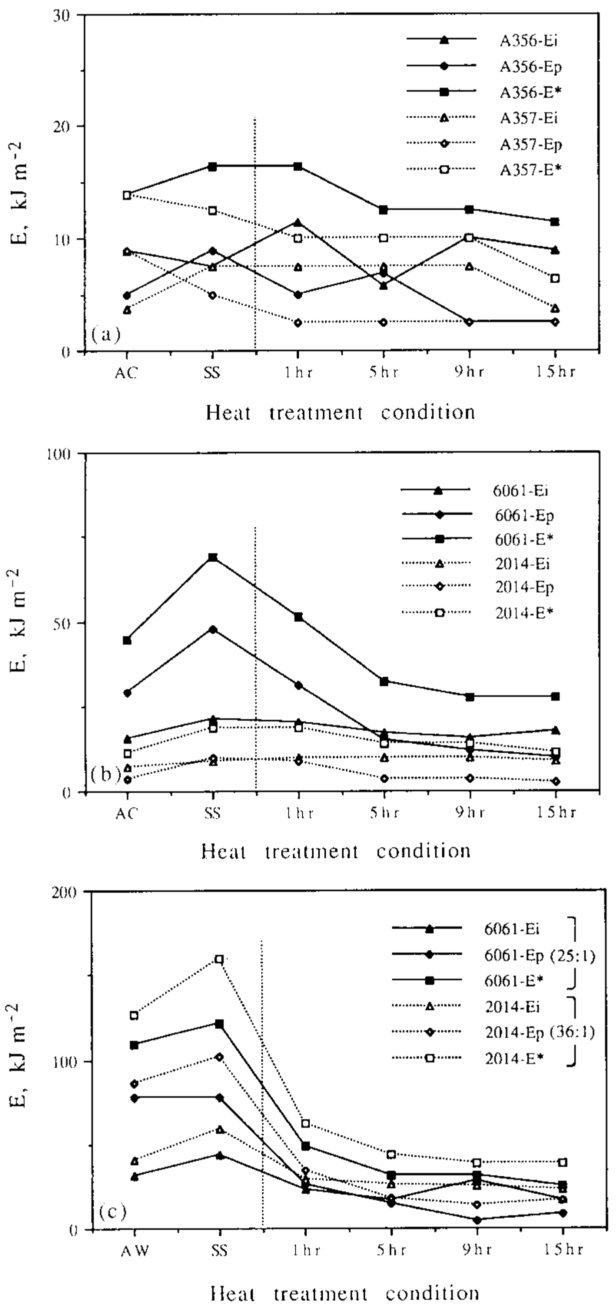

E^* is total fracture energy, which is sum of initiation energy E_i and propagation energy E_p

5 Variation of Charpy V-notch fracture energy with heat treatment for *a, b* as cast and *c* as worked composites

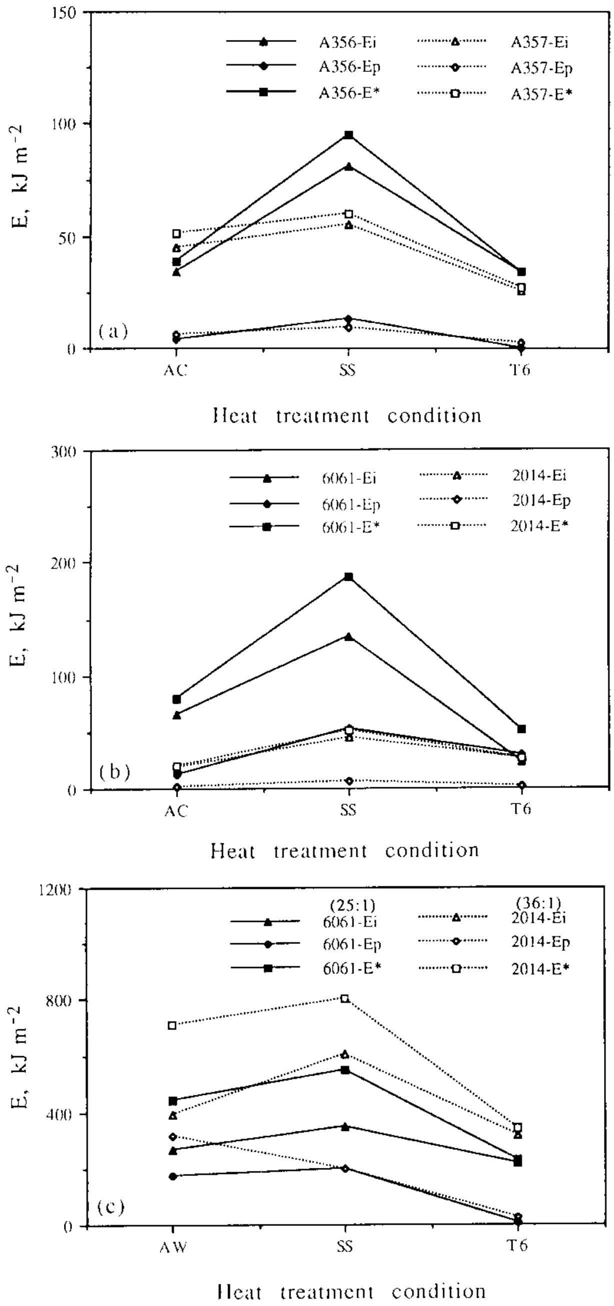

6 Variation of Charpy fracture energy, obtained using unnotched specimens, with heat treatment for *a, b* as cast and *c* as worked composites

CHARPY IMPACT TESTS

Typical responses from the Charpy V-notch tests for the four composites are shown in Fig. 4*a*. The fracture energy values were generally very low. The values of impact peak load F_p for each composite, though perhaps not precise, also suggest the classification of underaged and overaged conditions, and were seen to follow the same trend as the hardness measurements. Figure 5 shows the variation of fracture energy for the four composites. No trend is apparent. In some composites, e.g. A356, A357, and 2014, the total energy fell to $<10\ \mathrm{kJ\ m^{-2}}$, thus making the variation of fracture energy rather difficult to evaluate since such energy levels are beyond the resolution power of the testing machine. Nevertheless, it can be seen in Figs. 5*b* and 5*c* for the 6061 and/or 2014 composites that, in general, the total fracture energy decreased rapidly with thermal aging. This is mostly caused by the loss of propagation energy; the initiation energy component did not vary significantly. It appears that the increase in peak strength in the artificially aged composites due to the strengthening effect from the matrix results in much more drastic failure once microcracks are initiated.

To reveal a clearer variation of the fracture energy as a function of hot working and thermal treatments, systematic impact tests were performed primarily on the unnotched Charpy specimens. This significantly increases the initiation energy. Figure 4*b* shows typical response curves. For the A356 and A357 composites the variation of total fracture energy with heat treatment is almost exclusively governed by the initiation energy, as shown in Fig. 6*a*. In these two as cast composites, E_i should be mostly imparted by the plastic deformation of the matrix, which itself is not

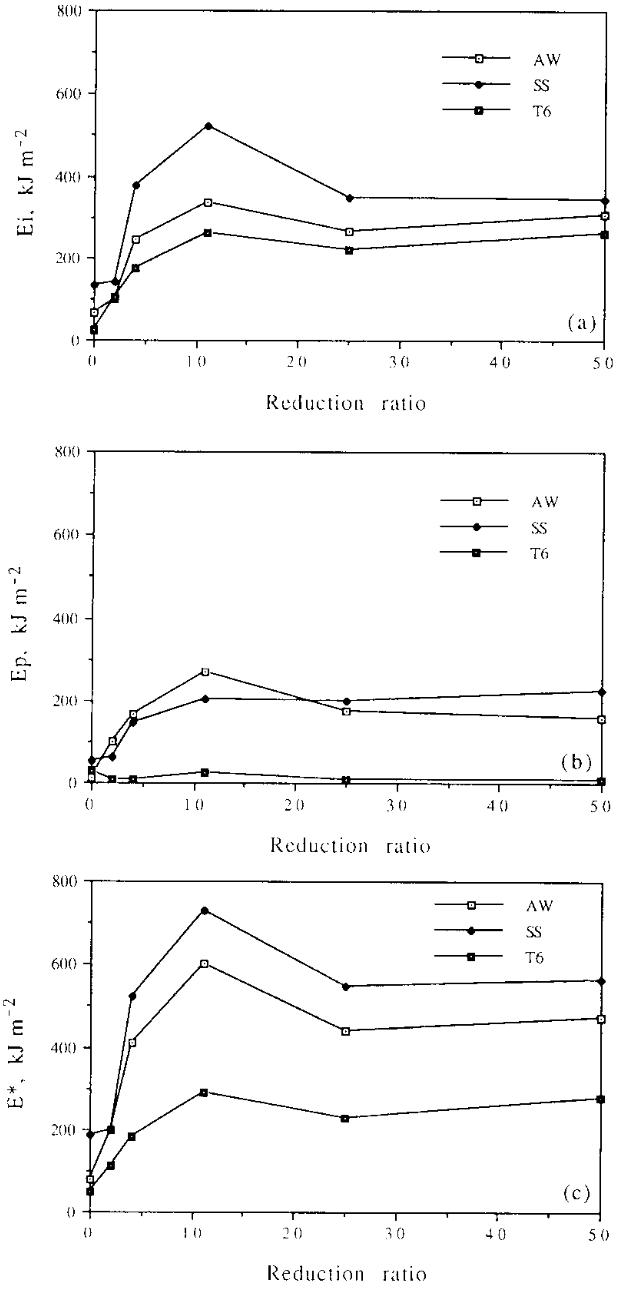

a E_i; *b* E_p; *c* E^*

7 Dependence of unnotched Charpy fracture energy on hot working reduction ratio for 6061–Al_2O_3 composites

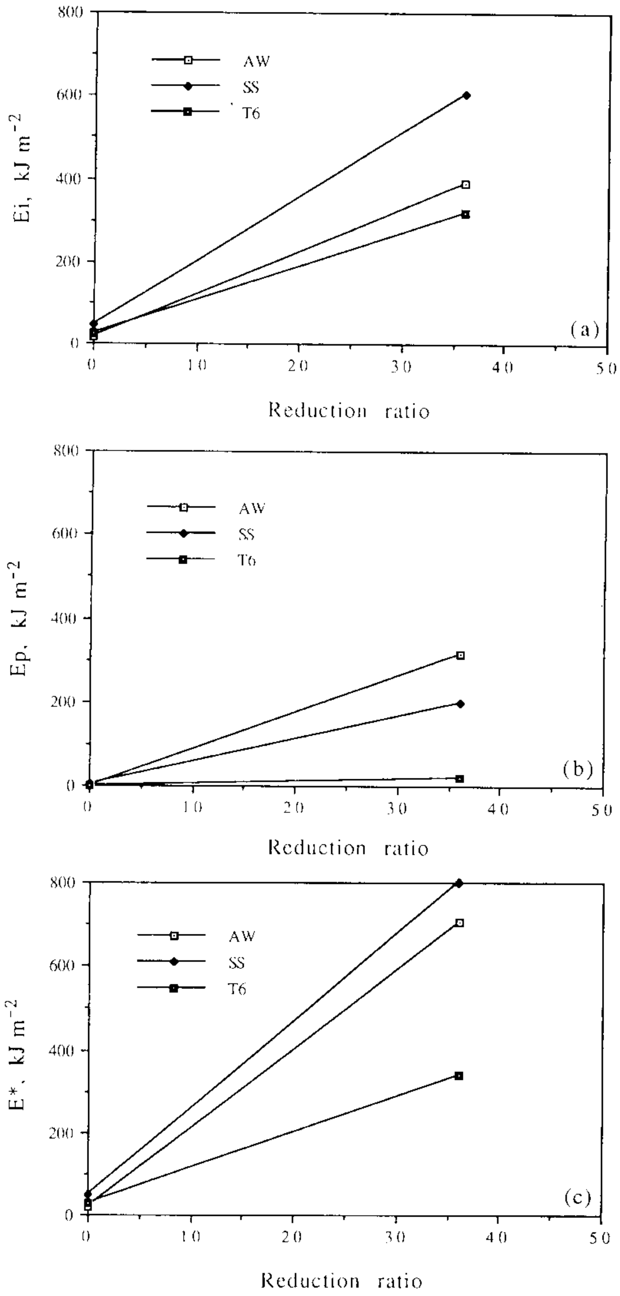

a E_i; *b* E_p; *c* E^*

8 Dependence of unnotched Charpy fracture energy on hot working reduction ratio for 2014–Al_2O_3 composites

pronounced, judging by the fractography. In comparison, the fracture energy of the A357 composite was consistently lower than that of the A356 composite, independent of the test method (Charpy notched or unnotched) and heat treatment (AC, SS, or T6), as shown in Figs. 5*a* and 6*a*.

The dependence of the Charpy fracture energy on thermal treatments for the unnotched 6061 composite specimens (Figs. 6*b* and 6*c*) is similar to the trend seen in the notched tests. The total fracture energy E^* for the extruded 6061 composites (25:1) in the T6 condition has increased to 230 kJ m^{-2} for the unnotched specimens, compared with 31 kJ m^{-2} for the notched specimens. The clearer trend revealed from the unnotched tests was the dependence on extrusion and/or rolling. Independent of the heat treatment condition of the specimens, the 6061 composite was found to possess the highest total fracture energy in specimens hot worked to a reduction ratio of 11:1, as shown in Fig. 7. These values of total fracture energy were comprised mainly of the initiation energy contribution, with the propagation energy having a less pronounced effect. The maximum value of E^* achieved for unnotched specimens of 6061 composite in the T6 condition was 290 kJ m^{-2}.

The 2014 composite was subjected only to an extrusion reduction ratio of 36:1. The dependence of (unnotched) Charpy fracture energy on heat treatment is shown in Figs. 6*b* and 6*c* and the change of fracture energy after extrusion is shown in Fig. 8. It can be seen that extrusion has significantly enhanced the toughness of the composite: the total fracture energy increased from 20 kJ m^{-2} for the AC specimens to 706 kJ m^{-2} for the AW specimens, a factor of 35. Even in the peak aged (T6) condition, the extruded 2014 composite exhibited $E^* = 341$ kJ m^{-2} for the unnotched test.

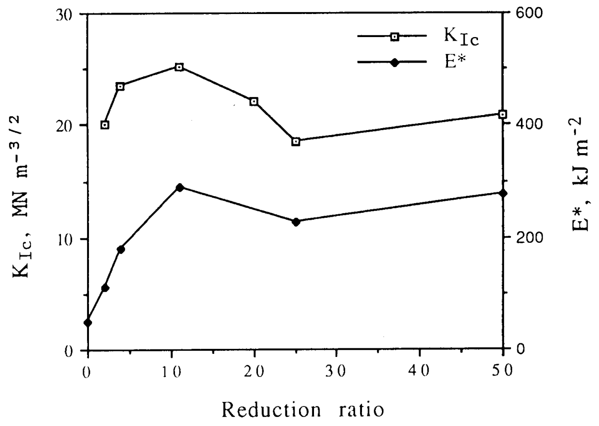

9 Variation of fracture toughness K_{Ic} with hot working reduction ratio for 6061–Al_2O_3 composite in T6 condition: data on E^* are included for comparison

MEASUREMENTS OF FRACTURE TOUGHNESS K_{Ic}

The results of the K_{Ic} tests as a function of aging condition and material system are given in Table 4. For the more brittle A356 and A357 composites, the K_{Ic} values for the AC and T6 specimens differed only slightly, consistent with the fracture energy tests (Figs. 5*a* and 6*a*). The A357 composite was observed to have a lower value of K_{Ic} than the A356 composite; both values are considerably lower than those for the unreinforced alloys.

Some of the K_{Ic} tests for the as worked 6061 composites did not meet the ASTM requirements; the data obtained can only be regarded as K_Q. From the valid data for the T6 temper, the sample extruded to 11:1 also has the highest K_{Ic} (25·2 MN m$^{-3/2}$), a trend consistent with the fracture energy tests, as shown in Fig. 9. It is worth mentioning that this value of K_{Ic} is already a great improvement for a cast MMC hot worked and aged to the T6 condition.

FRACTURE SURFACE EXAMINATIONS

On cross-sections of the fracture surface, especially for the Charpy V-notched specimens, differences are apparent at the front (near the notch), centre, and rear. In the present paper, the emphasis is on the surface morphologies of the central region of unnotched Charpy specimens. Figures 10*a*–10*d* are typical fractographs of the A356 and A357 composites. For these composites, the fracture surfaces of the AC and T6 specimens contain both cracked and decohered SiC particles, but interfacial decohesion is more

Table 4 Summary of measured fracture toughness K_{Ic}, MN m$^{-3/2}$

Material	Reduction ratio	AC/AW	T6	Ref. no.
A356 alloy	...	...	38·4*	1
A356–SiC	...	17·1	16·5	...
A357 alloy	...	41·7	26·7	23
A357–SiC	...	13·7	12·5	...
6061 alloy	...	...	37·0	24
6061–Al_2O_3	2:1	11·7*	20·0	...
	4:1	11·9*	23·5	...
	11:1	...	25·2	...
	20:1	...	22·0†	...
	25:1	13·4*	18·5	...
	50:1	11·7*	20·8	...
2014 alloy	...	...	24·2	25
2014–Al_2O_3	20:1	...	19·1†	...

* K_Q value, not satisfying ASTM E399 requirements.
† Data from specifications provided by Duralcan Company.

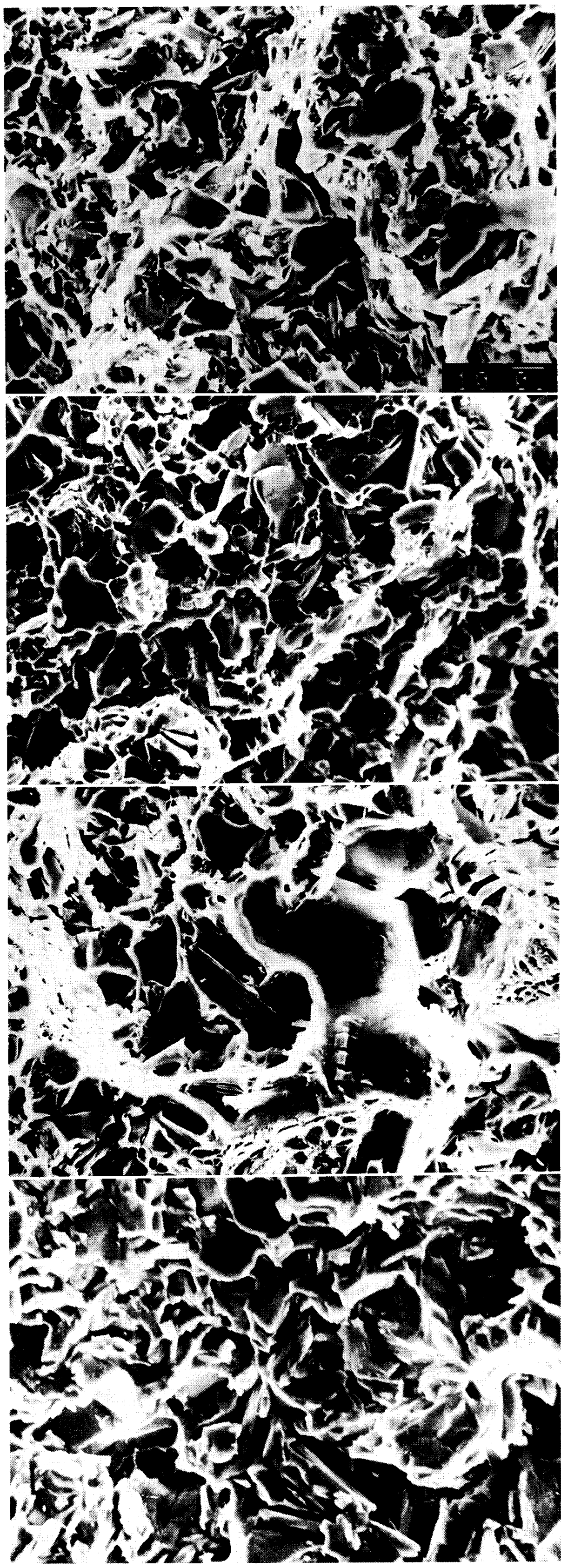

a b c d

A356–SiC in *a* AC and *b* AC + T6 conditions
A357–SiC in *c* AC and *d* AC + T6 conditions

10 Fractographs of unnotched Charpy specimens (SEM)

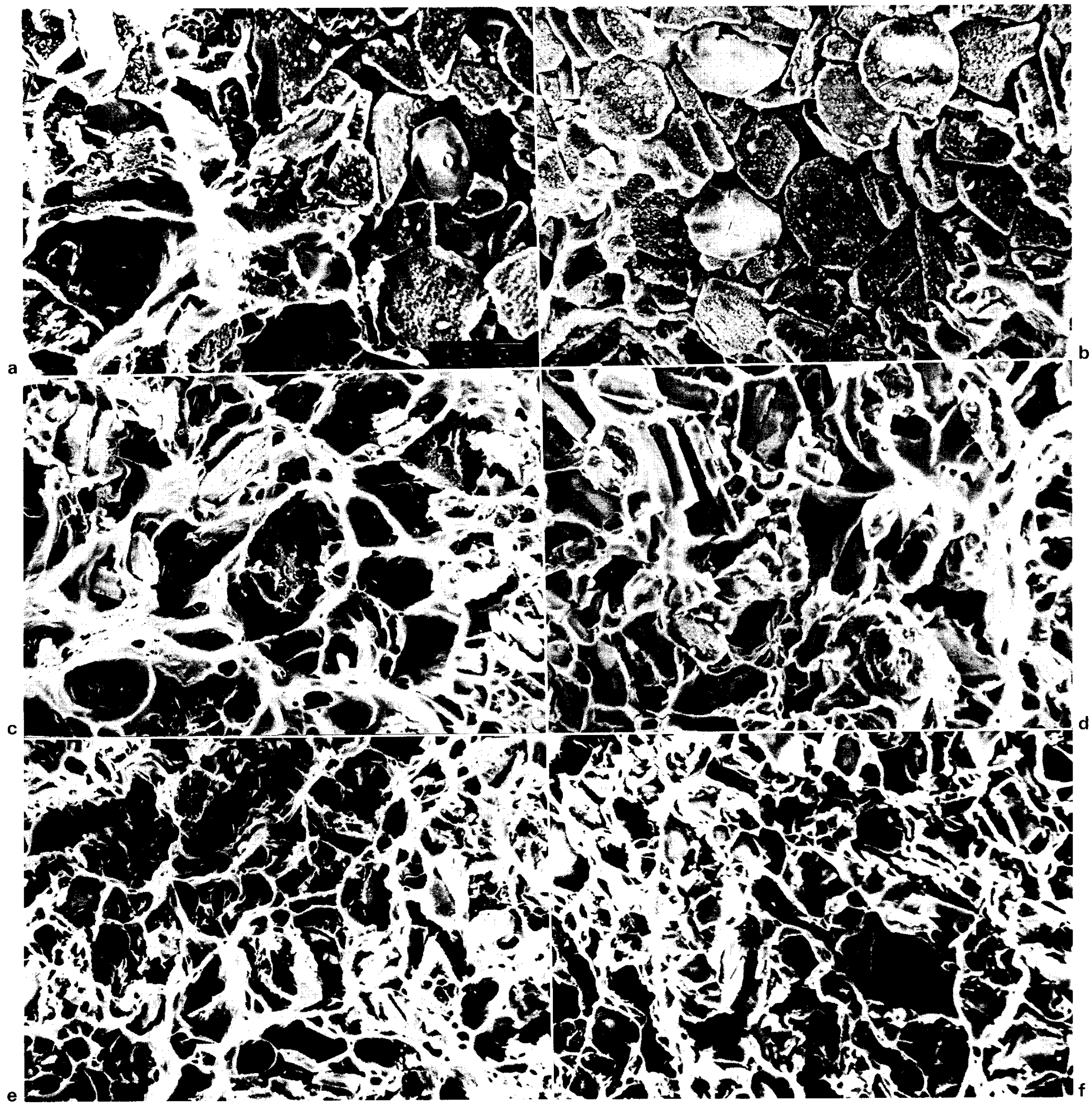

a AC; *b* AC + T6; *c* AW (11 : 1); *d* AW (11 : 1) + T6; *e* AW (50 : 1); *f* AW (50 : 1) + T6

11 Fractographs of unnotched Charpy specimens of 6061–Al_2O_3 composite (SEM)

pronounced in the T6 sample. Some of the SiC particles can be seen to be covered by the deformed matrix. Small equiaxial dimples (1–5 μm) can be observed in the matrix of both composites, but the matrix plastic deformation in the A356 composite is more evident.

Figure 11 shows the fracture surface of the 6061 composite. Severe clustering can occasionally be seen in the AC and AC + T6 samples, and extensive debonding and small spinel phases on the decohered Al_2O_3 particles can be seen in Figs. 11*a* and 11*b* (for both the AC and T6 conditions), suggesting weak particle–matrix bonding. As the reduction ratio of hot working increased, particle cracking was initiated and finally became the dominant fracture mode. The matrix also shows an increased tendency for dimple formation with increasing amount of working. At reduction ratios exceeding 11 : 1, there are many large and small dimples present in the matrix: the larger dimples are associated with the Al_2O_3 particles and the small dimples are associated with the precipitates or inclusions. The dimples can be seen to be shallower in the T6 than in the AW samples. The 2014 composite has a similar fractographic morphology to the 6061 composite (cf. Figs. 11 and 12).

Discussion

INFLUENCE OF MATRIX ALLOY ON TOUGHNESS

It has been suggested that the toughness of a MMC is influenced by the ductility of the base matrix;[10,11] thus the choice of matrix alloy is a crucial factor. Comparing A356 and A357 composites, which exhibit similar behaviour, it is consistently observed that the Charpy fracture energy of the A356 composite (notched or unnotched) is slightly higher. This trend was reflected in the K_{Ic} measurements and fracture surface examinations. The present results, coupled with the report[12] that the tensile elongations of A356 and A357 alloys cast in a permanent (or sand) mould

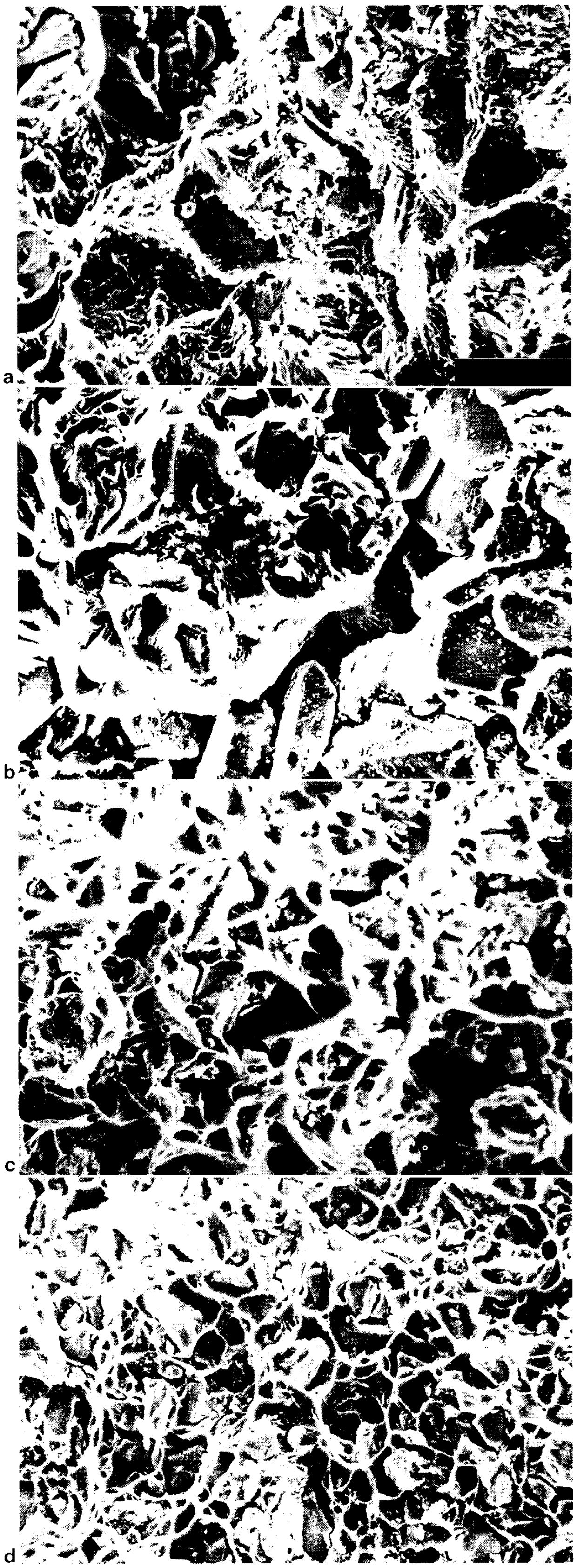

a AC; *b* AC + T6; *c* AW (36 : 1); *d* AW (36 : 1) + T6

12 Fractographs of unnotched Charpy specimens of 2014–Al_2O_3 composite (SEM)

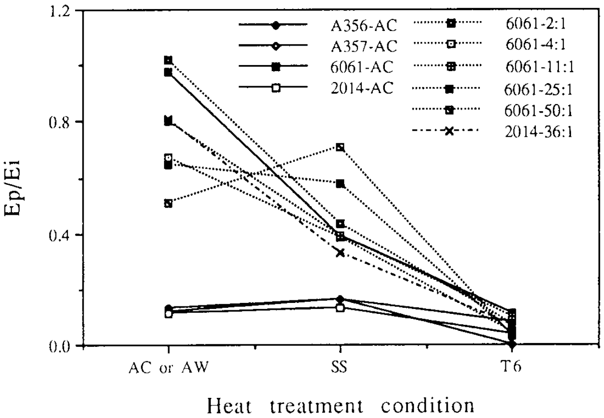

13 Dependence of ductility index (E_p/E_i) on heat treatment for composites subjected to different hot working processes: considerable decrease for AW specimens is mainly due to loss of E_p and less pronounced variation for AC specimens is due to slight decrease of E_i, with E_p virtually unaffected

are 10 and 5% (or 6 and 3%) respectively, suggest a strong influence of matrix ductility on the MMC toughness. The lower ductility in the A357 alloy is thought to be related to the addition of beryllium: the formation of BeO_2 results in higher strength and lower toughness.

Since the 6061 and 2014 composites possess the same size and volume fraction of Al_2O_3 reinforcement, these two systems can also be compared. The 6061 alloy, which is strengthened mainly by Mg_2Si, is not normally a high strength aluminium alloy, compared with the 2014 alloy used in aircraft, which is strengthened by the Guinier–Preston zone, θ series phases. It has been demonstrated[12] that the 2014 alloy, to either O or T6 temper, is always less ductile but stronger than the 6061 alloy. It follows that the 2014 composite usually exhibits lower toughness, except when subjected to a high level of hot extrusion. The latter result was found to be due to the more uniform distribution of particles, as is discussed below.

EFFECTS OF HEAT TREATMENT

There has been much discussion of the influence of thermal treatment, especially aging, on the fracture toughness of particle reinforced aluminium composites.[2,13–16] The toughness was generally observed to decrease with increasing aging time,[13,15,16] but in some cases it was found to remain almost constant.[15] The fracture mode was mostly dominated by particle cracking,[13,16] but particle debonding, which occurs mainly in overaged specimens, has also been documented.[2,14,15] The effect of thermal treatment has not been generalised: reports of the response of these composites differ.

In the present study, the total Charpy fracture energy was separated into the initiation and propagation contributions. It was observed that brittle fracture of a strong composite tends to have large E_i and small E_p. The reverse is found for ductile fracture of a softer material. To characterise such differences in fracture mode, a ductility index (DI)[17] can be defined as

$$DI = E_p/E_i \quad (1)$$

The higher the index, the more ductile is the composite. The variations of ductility index for the four composites based on the more reliable results obtained using Charpy unnotched specimens are shown in Fig. 13, in which it can be seen that, for the worked composites, the index decreases from the SS to T6 condition, implying a gradual approach to brittleness. This is predominantly caused by the rapid decrease of propagation energy; the initiation energy did not vary significantly. Peak aged composite specimens, once a critical amount of microcracking has taken place (corresponding to the occurrrence of peak load), will fail rapidly. The propagation energy for the T6 specimen is usually one-tenth of the initiation energy. The present results are consistent with most previous reports.[13,15] In contrast to the AW results, the less pronounced variation for the AC composite specimens is due to the slight decrease of E_i, with E_p virtually unaffected.

By examining the fractographs of the AC (or AW) and T6 specimens, it has been found that (i) the dimples in the T6 specimens tend to be shallower and smaller, indicating the increasing brittleness of the matrix with aging; and (ii) there is a noticeable increase in the amount of particle cracking in the T6 specimens, suggesting that the particle–matrix bond strength increases with aging. These observations imply that the loss of propagation energy due to thermal aging is caused partly by the strengthening but embrittling of the matrix and partly by more effective bonding. Since the composites are all particle reinforced, toughening by debonding should be a minor effect. Most of the fracture energy is contributed by the matrix plastic deformation. Once the matrix becomes more brittle, as in the T6 condition, the composite in turn becomes brittle. The fracture mechanisms of these composites were observed to be broadly similar. For unnotched Charpy specimens, the matrix first undergoes plastic deformation upon loading. At maximum load, the particles start to crack or debond according to their bonding strength, and this is followed by dimple formation which corresponds to the propagation process. The level of propagation energy is also determined by the susceptibility of the matrix to plastic deformation, and so the morphology of dimples can be an index of ductility.

The K_{Ic} data on A356 and A357 composites also suggest that heat treatment has the same effect: the values in the T6 condition are lower than those in the AC condition. Data on the 6061 composites cannot be used to evaluate this effect. In general, the toughness of MMCs is reduced as aging proceeds. Exceptions can occur when there are extensive interfacial reaction products with severe volume change during prolonged overaging, which reinduces debonding.

EFFECTS OF HOT WORKING

The influence of processing on the toughness has been studied by a number of investigators.[18-20] It was found that extrusion can enhance ductility and hot isostatic pressing can improve strength and modulus.[18] The present study is concentrated on the effect of extrusion (or rolling) reduction ratio. Other factors, e.g. working speed, temperature, or lubrication, remain fixed and are not considered here.

Figures 7 and 8 illustrate the marked improvement of the fracture energy of the 6061 and 2014 composites: its value can increase by eight times through appropriate working. On the basis of microstructural characterisation, such working should achieve:

(i) elimination of residual pores and defects formed during casting
(ii) much more uniform distribution of the reinforcing particles
(iii) stronger bonding between the matrix and particles
(iv) a more ductile matrix which might result from the homogenisation and refinement of grains during working.

The variation of the fracture energy with reduction ratio for the 6061 composite, as shown in Fig. 7, indicates a maximum at a ratio of 11 : 1. This result is corroborated by the K_{Ic} results. Because the working ratio is low, particle redistribution and bond strengthening have not yet reached a satisfactory level. For a reduction ratio of 11 : 1, the Al_2O_3 particles were seen to crack mostly during Charpy loading and there were some indications of debonding. When debonding occurs, it provides a crack blunting mechanism, which acts locally to arrest crack advancement. This can result in more local matrix deformation and microvoid formation, contributing to the highest fracture energy. When the reduction ratio was increased to 25 : 1 or 50 : 1, debonding was progressively rare. The Al_2O_3 particles were predominantly seen to crack. It follows that optimum toughness will correspond to an optimum bond strength; lower or higher strengths will lead to lower toughness. In addition, the slight decrease of toughness at high reduction ratio (25 : 1 and 50 : 1) might also be due to the more extensive particle damage (complete or partial cracking of the Al_2O_3 particles) caused by the heavier working. The precrack inside the composite provides an easier path for premature failure, which will result in lower toughness.

It is noted that the Al_2O_3 particles in worked composites are not only redistributed but also smaller. Table 2 gives the resulting particle size and calculated interparticle spacing L_s. Since the 6061 matrix is softer than the 2014 matrix, the fragmentation force from the matrix acting on the particles during extrusion or rolling is thought to be lower in the 6061 composite. The fragmentation effect makes the total particle number density higher and the interparticle spacing smaller. Previous research[1,21] has suggested that higher toughness will be obtained in composites having larger particle size and interparticle spacing for the same volume fraction. This may be attributed to the larger space for the matrix dislocations to accommodate the deformation. The present result, judging only from the interparticle spacing, seems not consistent with the previous statements. However, it should be noted that the overall variation of particle size and spacing is not more than 50%, which is considerably less than in previous work, where the particle size varied from 25 to 120 μm.[1] In fact, Flom and Arsenault[21] have found that K_{Ic} was independent of particle size for particles less than 20 μm in size. The improvement in toughness by particle redistribution in the present work appears to have overshadowed the influence from the small variation of particle size and spacing.

Based upon the above analyses, it can be seen that the fracture mechanisms of MMCs may vary significantly depending on the processing and heat treatment history. The interfacial bond strength might differ markedly in specimens in the AC lightly worked or heavily worked condition. This also applies in the AW + T6 specimens, in which case the bond strength is sometimes altered by the solution and aging treatments. Furthermore, particle clustering and redistribution can be significantly affected by working, resulting in different fracture modes. These might account for the discrepancy in MMC fracture mechanisms reported in the literature.[2,13-16]

NOTCH SENSITIVITY

The notch sensitivity is an important parameter for practical applications, especially when safety factors are of concern. The notch sensitivity index (NS) can be defined as

$$NS = E^*_{unnotched}/E^*_{CVN} \quad (2)$$

where $E^*_{unnotched}$ and E^*_{CVN} are the total Charpy fracture energy measured using unnotched and V-notched specimens, respectively. The values obtained for the present composites in various conditions are given in Table 5. The brittle AC composite specimens show a much lower notch sensitivity than the tougher worked composites. This is thought to be because the AC composite is already extremely brittle and possesses regions of high stress

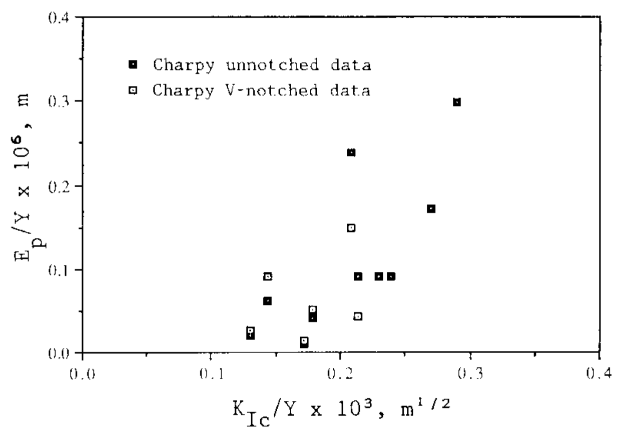

14 Relationship between E_p (V-notched and unnotched) and K_{Ic}, normalised by elastic (Young's) modulus *Y*, for all composites studied

concentration, such as the areas containing numerous particle clusters separated by 'microgaps'. Parts of these regions may already have levels of stress concentration close to that which results from the externally applied V-notch. In contrast, the composite extrudates, such as the 6061 composite extruded to 25:1 reduction, exhibit marked notch sensitivity, since the materials have intrinsically a more uniform microstructure and stress distribution. This indicates that the toughness of MMCs can be affected by surface roughness.

RELATIONSHIP BETWEEN E^* AND K_{Ic}

From the limited data on K_{Ic}, E^*, E_i, and E_p, it can be seen that the variations of K_{Ic} and E^* (or E_i, E_p) as a function of heat treatment or reduction ratio are similar. This might suggest a relationship between the two parameters, despite the difference in loading condition and stress state. Attempts to correlate E^* and K_{Ic} have been reported previously,[7,8] mainly for steels. To the authors' knowledge, the application to more complex materials, such as MMCs, has not been attempted. The physical meaning of E^* and K_{Ic} is different, but the terms are both used to characterise toughness. First, the loading stress state is dissimilar. Secondly, E^* represents the total energy absorbed and K_{Ic} measures the highest resistant force at the onset of crack propagation. Finally, test conditions are dynamic for the former, but quasistatic for the latter, so comparisons can be made only on materials exhibiting little or no strain rate sensitivity.[22] Notwithstanding these differences, the two parameters reveal similar toughness trends and both are highest at an extrusion ratio of 11:1 for the 6061 composite.

Since the specimens for K_{Ic} measurements have been precracked by fatigue, the value of K_{Ic} should be related more to the crack propagation than to the crack initiation. This applies particularly for the unnotched specimens in which a large portion of initiation energy is due to plastic deformation of the matrix and microcrack formation near the interface. It is therefore expected that some relationship might be established between the K_{Ic} and E_p data, not necessarily of physical meaning, but simply for practical usefulness, since the measurement of one might give an estimate of the other.

Figure 14 shows the relationship between K_{Ic} and E_p for Charpy notched and unnotched specimens: both parameters have been normalised by the elastic modulus to eliminate the difference in modulus among the four composites. Since the data on K_{Ic} are limited, the trend is not definite. However, although an empirical relationship cannot be established from the present study, it can be stated that a tougher composite should have higher values of fracture energy and fracture toughness. The two parameters might be complementary: in the present study, if K_{Ic} increases, both E_p and E_i, and therefore E^*, will increase.

Table 5 Notch sensitivity* of composites studied

			6061 Al_2O_3		2014 Al_2O_3	
Condition	As cast A356 SiC	As cast A357 SiC	As cast	Worked (25:1)	As cast	Worked (36:1)
AC/AW	2·83	3·69	1·78	4·04	1·77	5·59
SS	5·83	4·80	2·71	4·51	2·70	5·03
T6	3·01	3·07	1·85	7·25	1·96	8·79

* Obtained using equation (2).

Conclusions

1. The toughness characterised in terms of fracture energy and fracture toughness measurements is basically consistent. The most important factors governing the toughness of particle reinforced metal matrix composites (MMCs) are the toughness of the matrix alloy and the distribution of particles.
2. The fracture energy tends to decrease markedly with increasing aging time, from the underaged to the overaged condition. The decrease in total fracture energy E^* was found to be caused mainly by the drastic reduction of propagation energy E_p; the initiation energy E_i did not seem to be affected by artificial aging.
3. Hot extrusion or rolling can lead to (i) elimination of residual pores and defects formed during casting; (ii) much more uniform distribution of the reinforcing particles; (iii) stronger bonding between the matrix and particles; and (iv) a more ductile matrix resulting from the homogenisation and refinement of grains during working. This will markedly improve the toughness, mainly through the increase of initiation energy.
4. The optimum level of hot working of MMCs is the level required to achieve uniform particle distribution and optimum bond strength.
5. The tougher MMCs also have higher notch sensitivity, which will be of concern if the surface is not sufficiently smooth.
6. Although an empirical relationship between fracture energy and fracture toughness has not been definitely established, it can be stated that a tougher composite should exhibit higher values for both. The two parameters might be complementary: it was found that if K_{Ic} increases, then so do E_p, E_i, and, therefore, E^*.

Acknowledgements

The authors wish to express their gratitude to Dr Y. C. Chen at the Industrial Technology Research Institute of Taiwan for providing the materials. The work was sponsored by the National Science Council of Taiwan.

References

1. J. J. STEPHENS, J. P. LUCAS, and F. M. HOSKING: *Scr. Metall.*, 1988, **22**, 1307–1312.
2. N. HAN, G. POLLARD, and R. STEVENS: *Mater. Sci. Technol.*, 1992, **8**, 52–56.
3. S. V. KAMAT, J. H. HIRTH, and R. MEHRABIAN: *Acta Metall.*, 1989, **37**, 2395–2402.
4. P. N. KALU and T. R. McNELLEY: *Scr. Metall.*, 1991, **25**, 853–858.

5. J. J. LEWANDOWSKI and C. LIU: *Mater. Sci. Eng.*, 1989, **A107**, 241–255.
6. C. M. FRIEND: *Mater. Sci. Technol.*, 1989, **5**, 1–7.
7. J. M. BARSOM and S. T. ROLFE: 'Impact testing of metals', STP 466, 281–288; 1970, Philadelphia, PA, ASTM.
8. R. ROBERTS and C. NEWTON: Bulletin 265, Welding Research Council, Cambridge, February 1981.
9. M. FERRY, P. MUNROE, A. CROSKY, and T. CHANDRA: *Mater. Sci. Technol.*, 1992, **8**, 43–51.
10. D. L. DAVIDSON: *Metall. Trans.*, 1991, **22A**, 113–123.
11. Z. WANG and R. J. ZHANG: *Metall. Trans.*, 1991, **22A**, 1585–1593.
12. 'Aluminum – properties and physical metallurgy' (ed. J. E. Hatch); 1984, Metals Park, OH, ASM.
13. T. F. KLIMOWICZ and K. S. VECCHIO: in 'Fundamental relationships between microstructures and mechanical properties of metal–matrix composites', (ed. P. K. Liaw and M. N. Gungor), 255–267; 1990, Warrendale, PA, TMS.
14. C. P. YOU, A. W. THOMPSON, and I. M. BERNSTEIN: *Scr. Metall.*, 1987, **21**, 181–185.
15. M. MANOHARAN and J. J. LEWANDOWSKI: *Scr. Metall.*, 1989, **23**, 301–304.
16. M. MANOHARAN and J. J. LEWANDOWSKI: *Acta Metall.*, 1990, **38**, 489–496.
17. D. F. ADAMS: in Proc. 4th Conf. on 'Composite materials: testing and design', 409–426; 1977, STP 617, Philadelphia, PA, ASTM.
18. A. H. NAKAGAWA and M. N. GUNGOR: in 'Fundamental relationships between microstructures and mechanical properties of metal–matrix composites', (ed. P. K. Liaw and M. N. Gungor), 127–143; 1990, Warrendale, PA, TMS.
19. T. R. McNELLEY and P. N. KALU: *Scr. Metall.*, 1991, **25**, 1041–1046.
20. A. NIKLAS, L. FROYEN, and L. DELAEY: *Mater. Sci. Eng.*, 1991, **A135**, 225–229.
21. Y. FLOM and R. J. ARSENAULT: *Acta Metall.*, 1989, **37**, 2413–2423.
22. R. W. HERTZBERG: 'Deformation and fracture mechanisms of engineering materials', 3 edn, 341; 1988, New York, Wiley.
23. A. BLOYCE and J. C. SUMMERS: *Mater. Sci. Eng.*, 1991, **A135**, 231–236.
24. D. F. HASSON and C. R. CROWE: in Proc. Conf. 'Strength of metals and alloys', 1515–1520; 1985, Oxford, Pergamon.
25. R. W. HERTZBERG: 'Deformation and fracture mechanisms of engineering materials', 3 edn, 304; 1989, New York, Wiley.